EXPLOITING NON-GAUSSIAN PHASE DISTRIBUTIONS TO MODEL MICRON-SCALE RESTRICTED DIFFUSION

Leigh A. Johnston[1,2], David Wright[2,3], and Iven M. Mareels[1]

[1]*NeuroEngineering Laboratory, Electrical and Electronic Engineering, University of Melbourne, Parkville, VIC, Australia,* [2]*Florey Neuroscience Institutes, Parkville, VIC, Australia,* [3]*Centre for Neuroscience, University of Melbourne, Parkville, VIC, Australia*

INTRODUCTION: Diffusion imaging methods for inferring axon diameter distributions in mammalian white matter operate in a regime in which Brownian motion trajectories fully explore the restricted space between diffusion gradient encodings. That is, the diffusion time, Δ ms, cylinder radius, R µm, and diffusion coefficient, D µm^2/ms, relate as $\Delta >> R^2/D$. The AxCaliber model [1] derives from the multiple impulse propagator formalism [2] under the narrow pulse approximation. We recently proposed a probabilistic treatment based on the theory of extremes [3] to derive an analytic model of restricted diffusion that obviates the truncation of Bessel function expansions. For small R, however, this reduces to the quadratic form predicted by van Gelderen et al [4]. Thus the aim of the current study was to revisit the highly non-Gaussian phase characteristic of single-micron scale cylindrical compartments, to derive a model of restricted diffusion that is tailored to the axon-scale inference regime. We exploit the seminal work of [6] to derive a simple closed-form restricted signal decay model, and demonstrate its efficacy on two experimental datasets.

THEORY: For $\Delta >> R^2/D$, the 1-d Brownian motion trajectories fully explore the restricted space between gradient encodings. The resultant phase distribution under the narrow pulse approximation is spatially uniform, conditional on the trajectory's initial position. Integration over all initial positions results in a triangular phase distribution of twice the compartment width [6], giving rise to a sinc-squared signal decay function, $E_{res}(q,R)$ [5]. We parameterise the distribution of cylinder radii by a $\gamma(k,\theta)$-distribution. It is our conjecture that under these conditions, the restricted diffusion signal decay is a tractable integral, with closed-form solution,

$$E_{res}(q) = \int E_{res}(q,R)p(R)\,dR = \int \mathrm{sinc}^2(2Rq)\frac{R^{k-1}e^{-R/\theta}}{\theta^k\Gamma(k)}\,dR = \frac{1}{q^2}\left(1-\frac{1}{\left(1+4\pi^2\theta^2q^2\right)^k}\right). \quad (1)$$

The distribution of cylinder radii, $p(R)$, can be inferred from estimated $\{k,\theta\}$ from experimental $E(q)$ curves.

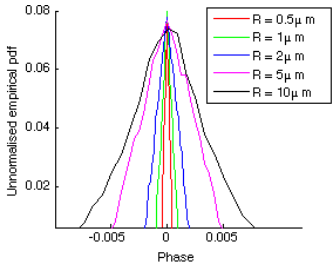

Fig.1 Triangular empirical phase distributions of width $\propto 2Rq$ from simulated restricted traiectories.

METHODS: Simulated PGSE data were generated by sampling 1-d Brownian motion trajectories restricted between plates separated by $2R$ via reflection at the boundaries. Sets of trajectories were generated for $R \in \{0.5,1,2,5,10\}$µm, g = 200 mT/m, Δ = 20 ms, and D_{free} = 2 µm^2/ms, from which phase histograms were formed. **Experimental datasets** were acquired on a Brüker 4.7T with BGA12S-HP gradient set, dw-EPI. **Dataset 1:** 8-week postnatal *ex vivo* sheep brain, TR/TE=3000/40ms, 16 shots, mid-sagittal slice, FOV = 6.4x6.4cm^2, matrix = 256x256, NEX=3, g={5,10,…,50,75,100,…,400}mT/m, δ=5ms, Δ={30,45,60}ms. Regions-of-interest (ROIs) were manually delineated in the corpus callosum, cortex and 4%PFA background as a control. **Dataset 2:** *Ex vivo* rat intact cochlea, auditory nerve surrounding tissue, imaged using a cryogenically cooled surface coil, TR/TE=3000/23ms, 16 shots, single 1mm slice perpendicular to auditory nerve fibres, FOV=1x1cm^2, matrix=128x128, NEX=4, g={5,10,…,50,75,100,…,400}mT/m, δ=5ms, Δ={20,40}ms. An ROI was manually delineated in the auditory nerve (Fig.2A). **Analysis:** All signal decay curves were normalised to remove Rician bias. For each ROI, a hindered/ restricted 2-compartment model $E = fE_{hind}+(1-f)E_{res}$, $0 \le f \le 1$, with $E_{hind}=\exp(-4\pi^2 d(\Delta-\delta/3)q^2)$, and E_{res} in Eq.(1), was optimised using nonlinear least squares. Estimated parameters were f, k, θ, and hindered ADC, d.

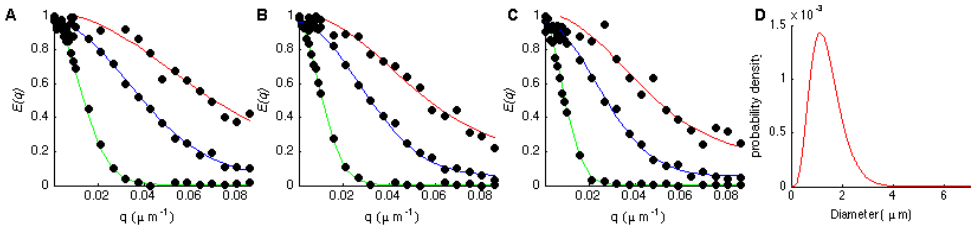

Fig.2 Ex vivo sheep brain signal decay curves in corpus callosum (red), cortex (blue) and fixative solution (green), for **A.** Δ = 30 ms, **B.** Δ = 45 ms, **C.** Δ = 60 ms. Black dots are experimental data-points, solid lines are estimated models. **D.** Inferred axon diameter distribution from corpus callosum estimated models in panels A-C.

RESULTS: The empirical distributions derived from simulated data (Fig.1) verify the triangular phase distribution with width proportional to the compartment size under the narrow pulse approximation. Imaging of the sheep brain dataset (Fig.3A-C) produced control curves (4%-PFA) with estimated hindered ADC of 3.0µm^2/ms, a hindered ADC in the cortex of 0.4µm^2/ms, and restricted diffusion in the corpus callosum for the axon diameter distribution (Fig.3D). The auditory nerve signal decay curve (Fig.2B) was well-fit by the two-compartment model, with a resultant axon diameter distribution (Fig.2C) with mean value 1.7µm in agreement with histology (1.7 +/- 0.5µm [8]).

CONCLUSION: We have derived a closed-form expression for restricted diffusion in axons as an alternative to the AxCaliber model [1], that combines the characteristic non-Gaussian phase distributions with a parametric distribution of axon diameters. The veracity of the model was demonstrated in application to two experimental datasets, inferring distributions that closely match histological gold standards. Important ongoing work includes consideration of permeable barriers [7] and relaxation of the narrow pulse approximation.

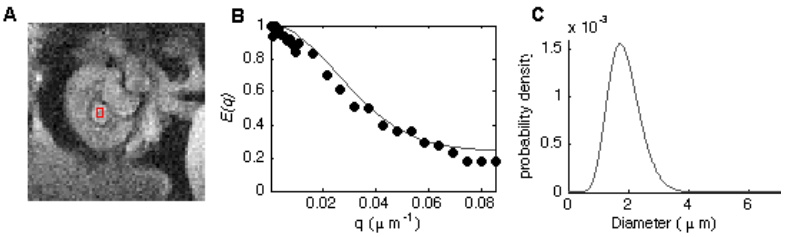

Fig.3 A. Auditory nerve ROI (red square) in ex vivo rat cochlea. **B.** Signal decay, $E(q)$, experimental (dots), and estimated (line). **C.** Inferred axon diameter distribution.

References: [1] Assaf *et al* (2008) *MRM* 59:1347-1354. [2] Codd & Callaghan (1999) *JMR*, 137:358–372. [3] _____ [4] van Gelderen *et al* (1994) *JMR-B* 103:255-260. [5] Assaf *et al* (2004) *MRM* 52:965-978. [5] Sukstanskii *et al* (2003) *MRM* 50:735–742. [6] Cory & Garroway (1990) *MRM* 14:435-444. [7] Barbary (1991) *Hearing Res.* 54:75-90. [8] Yablonskiiy & Sukstanskii (2010) *NMR Biomed.* 23:661-681.